Hypocenter Location via Hodogram Analysis of Noisy 3C Microseismograms

Joe Wong, Lejia Han, and John C. Bancroft
CREWES, University of Calgary

Summary

When the signal-to-noise ratios on three-component (3C) microseismograms are high, a method utilizing hodogram analysis and back-azimuth projection works well for mapping microseismic hypocenter locations in a homogeneous isotropic velocity field. However, when the signal-to-noise levels are low, the accuracy of such a mapping method decreases significantly. To suppress random noise on the raw microseismograms, we apply frequency-domain filtering, time-domain windowing, trace averaging, and signal-noise separation (NSS). After noise suppression, the back-azimuth method coupled with statistical averaging of raypath intersections produces reasonably accurate hypocenter locations.

Introduction

In reservoir stimulation of tight-gas plays, hydraulic fracturing is used to crack gas-bearing formations and increase the flow of gas into producing wells. As the rock formation cracks, microseisms or micro-earthquakes occur at the point of fracturing. Microseismic monitoring helps reservoir engineers evaluate the effectiveness of the stimulation by mapping microseism hypocenters and therefore the location and extent of the fracturing. The release of microseismic energy induced by hydraulic fracturing is generally weak, so that the associated microseismograms have low signal-to-noise ratios (SNRs).

Hodogram analysis of direct P-wave arrivals on 3C microseismograms is used to determine the propagation directions between 3C geophones in an observation well and the microseism hypocenter. Figure 1 shows that, for perfectly noise-free microseismograms in a homogeneous isotropic velocity field, back-projecting the azimuths and dip angles of the propagation vectors from multiple geophones results in a single intersection point that coincides with the hypocenter. When the 3C seismograms are contaminated by random noise, the intersection points of propagation directions for different pairs of geophones generally do not coincide, but will be scattered. The scattering becomes more severe as SNRs decrease. Using synthetic microseismograms, we developed methods for mitigating the effects of random noise and improve the accuracy of hypocenter location.

Synthetic Microseismograms

We assume a vertical observation well located at x=0m, y=0m in a homogeneous and isotropic P-wave velocity field (v=4000m/s). An array of twelve 3C geophones separated by 50m is placed in the well at depths ranging from 2000m to 2550m. We generated noisy synthetic seismograms for this array assuming a P-wave microseismic source located at x_s=400m, y_s=300m, and z_s=2150m. The amplitudes of the arrivals on the x-y-z components were scaled to account for spherical spreading and according to the direction cosines of the propagation vectors between the microseismic source and the geophones. Random Gaussian was then added to simulate different SNR levels.

Hodograms Derived from Noisy Microseismograms

Figure 2(a) shows the noisy synthetic 3C microseismograms for one geophone. The event arrivals are highlighted by the rectangle. Figure 2(b) and 2(c) show the hodograms in the x-y plane (map view) and z-r plane (section view) plotted using the data points within the rectangle.

The propagation directions (dip angle and azimuth) are shown on these hodograms. The red dotted lines show the true propagation directions of the incoming wave. The black dotted lines are the least-squares straight-line fits to component values in the x-y and z-r planes. The solid blue lines have directions estimated from the weighted averages of the slopes of vectors defined by x-y and z-r data pairs on the hodograms. It is clear that the weighted-average directions are closer to the true directions than the least-squares directions.

Noise Reduction

Figure 3(a) displays the noisy 3C microseismograms for all twelve geophones in the array. Figure 3(b) displays the same seismograms after noise reduction using bandpass filtering, time windowing, and a noise-signal separation (NSS) procedure. The NSS procedure involves time-picking and alignment of the traces of each component. The aligned traces of the component showing the best amplitudes are averaged to find a noise-reduced reference trace. The dot product of the normalized reference trace with each of the aligned 3C seismograms gives an amplitude coefficient. The coefficient is used to scale the reference trace and obtain a noise-reduced signal trace. The difference between the noise-reduced signal trace and the original trace should be a residual noise trace with little or no resemblance with the reference trace. NSS reduces random noise while largely preserving polarities and relative amplitudes of the analyzed traces. The preservation of polarities and relative amplitudes is essential for the hodogram method to give good estimates of the propagation directions.

Hypocenter Location

Figures 4(a) and 4(b) show the back-projection of propagation directions derived from the unprocessed noisy microseismograms on Figure 3(a). On the section view of Figure 4(a), the intersection points of pairs of dip directions are widely scattered, and the averages of the r-z coordinates of the intersections are far from the true r-z coordinates. On the map view of Figure 4(b), the azimuths span a large range of angles, but the average azimuth appears close to the true azimuth. The green circle is drawn with radius equal to the estimated r-coordinate from Figure 4(a). The x-y coordinates of the intersection of this circle with the line drawn in the direction of the average azimuth are far from the true source coordinates.

Figures 5(a) and 5(b) show the back-projection of propagation directions derived from the noise-reduced microseismograms on Figure 3(b). On the section view of Figure 5(a), the intersection points of pairs of dip directions are much more tightly clustered than those on Figure 4(a). The averages of the z-r coordinates of the intersections are reasonably close to the true z-r coordinates. On the map view of Figure 5(b), the azimuths span a small range of angles, and the average azimuth is almost equal to the true azimuth. The green circle is drawn with radius equal to the estimated r-coordinate from Figure 5(a). The x-y coordinates of the intersection of this circle with the average-azimuth line are close to the true source coordinates.

Conclusions

The hodogram-analysis and back-propagation method of locating microseismic hypocenters works well in a homogeneous and isotropic velocity field if the 3C seismograms have high SNRs. When SNRs are low, noise suppression techniques such as frequency filtering and noise-signal separation must be applied to the raw seismograms before performing hodogram analysis. Reasonably accurate estimates for the hypocenter coordinates can then be found by averaging the intersection points of estimated propagation vectors with dip angles and azimuths determined from hodogram analysis. Extensive testing of the technique using synthetic data from multiple 3C geophones in a single vertical observation well indicated that the method is able to give reliable estimates of hypocenter coordinates even when the raw 3C microseismograms have SNRs as low as 3.

Acknowledgement
We thank NSERC and the industrial sponsors of CREWES for supporting this research.

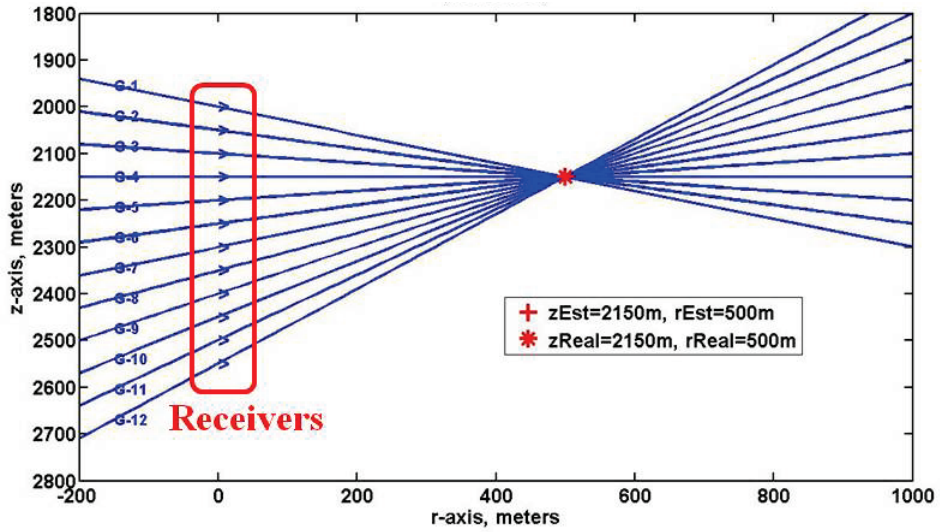

FIG. 1: Schematic diagram in section view showing back-propagation for hypocenter mapping using noise-free microseismic data. Blue lines are the back-projected propagation vectors determined from hodograms at the geophones. They intersect at one point that is exactly the hypocenter location.

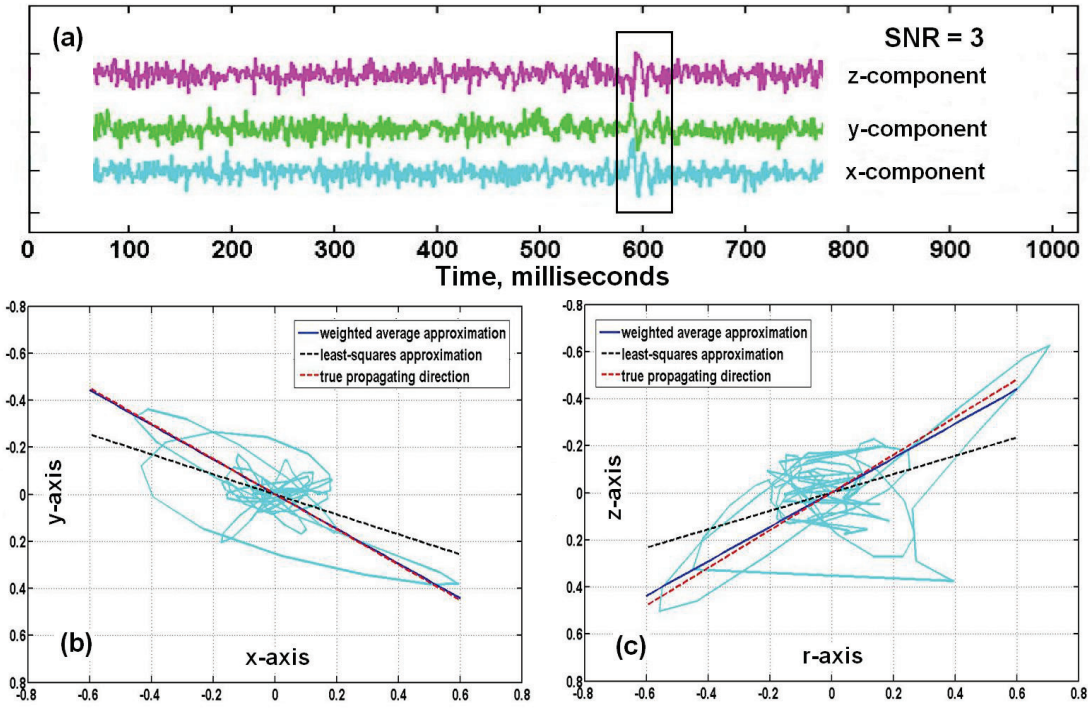

FIG. 2: (a) Synthetic noisy 3C seismograms with SNR=3 for one geophone; hodograms are defined by data points from the 3C seismic arrivals, i.e., points within the black rectangle; (b) the hodogram in the x-y plane defined by data points from the x and y components; (c) the hodogram in the z-r plane defined by data points from the z and r components.

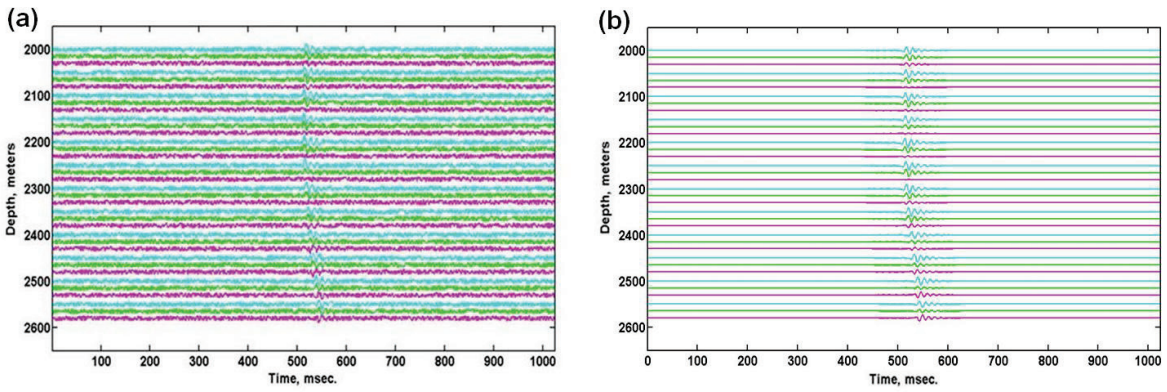

FIG. 3: (a) Synthetic noisy 3C seismograms with SNR=3 from twelve geophones; (b) noisy seismograms after processing to reduce random noise prior to hodogram/back-azimuth analysis; x-component traces are blue; y-component traces are green; z-component traces are pink.

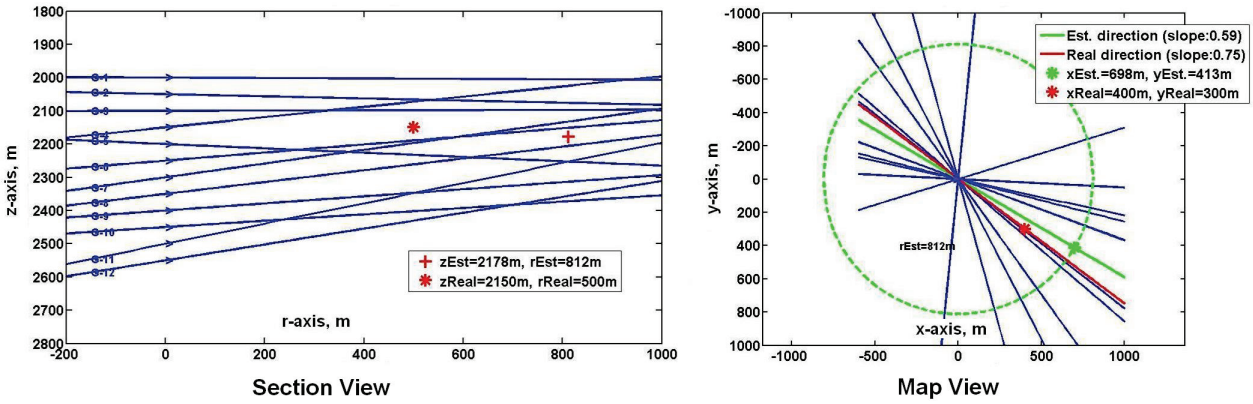

FIG. 4: Hodogram/back-azimuth analysis for the unprocessed noisy seismograms of Figure 3(a). The estimated hypocenter location is far from the true location.

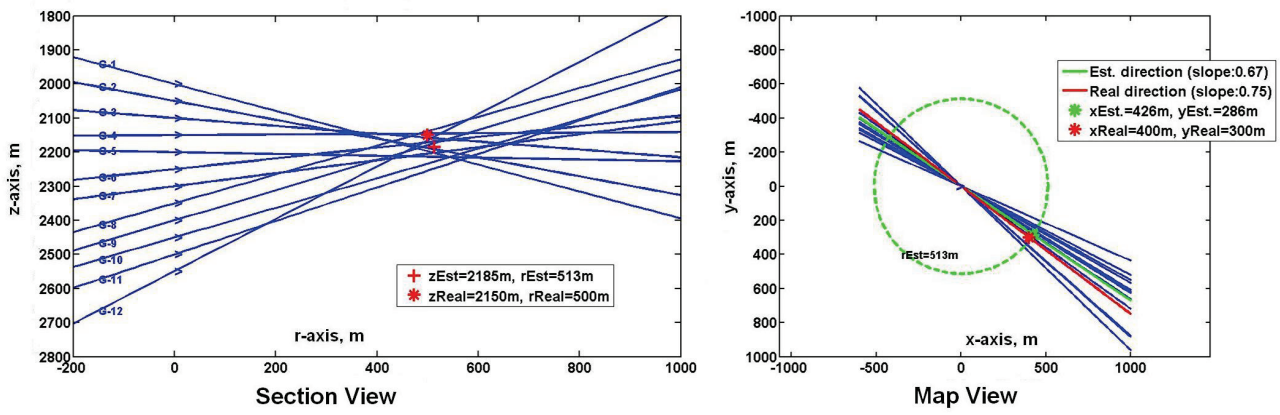

FIG. 5: Hodogram/back-azimuth analysis for the filtered, windowed, and noise-separated seismograms of Figure 2(b). The estimated hypocenter location is close to the true location.